JOURNAL OF COLLOID AND INTERFACE SCIENCE **208,** 49–62 (1998)
ARTICLE NO. CS985698

Preparation of Poly(methylmethacrylate) Microcapsules with Liquid Cores

Andrew Loxley and Brian Vincent[1]

School of Chemistry, University of Bristol, Cantock's Close, Bristol, BS8 1TS, United Kingdom

Received October 27, 1997; accepted May 31, 1998

Particles with liquid cores and solid shells have been prepared by the controlled phase separation of poly(methylmethacrylate) (PMMA) within the droplets of an oil-in-water emulsion. The oil phase of the emulsion contained poly(methylmethacrylate), a good solvent for the polymer (CH_2Cl_2), a poor solvent (hexadecane, decane, octanol, or tetrachloromethane), and in some cases acetone (a water soluble co-solvent) to aid emulsification. Emulsions were prepared using a Silverson high-speed stirrer, and the droplet size distributions were determined using a Coulter particle counter. Size distributions were found to be dependent on the nature of the emulsifier, the concentration of acetone in the oil phase, and the concentration of polymer in the oil phase. The good solvent was then removed under reduced pressure, causing the poly(methylmethacrylate) to phase separate within the emulsion droplets. The resultant two-phase particles were characterized by optical microscopy and scanning electron microscopy. Particle morphologies depended strongly on the nature of the non-solvent and also the emulsifier employed. Spreading coefficients were calculated from interfacial tension and contact angle measurements, and were used to account for the morphologies observed. Core/shell microcapsules were formed when hexadecane or decane was used as non-solvent, and only when polymeric emulsifiers were employed. All other combinations yielded "acorn"-shaped particles. The thickness of microcapsule walls was found to be a constant fraction of the overall capsule diameter for all microcapsule sizes and depended, as expected, on the concentration of polymer in the oil phase.

Key Words: **microcapsules; core/shell particles; phase-separation; spreading-coefficients.**

INTRODUCTION

The production of microparticles consisting of two immiscible polymers is of considerable practical interest. Several possible morphologies have been considered, some of which are summarized in Fig. 1. The heteroaggregate systems (Fig. 1d) may be observed where there are significant attractive forces between dissimilar colloidal particles (e.g., oppositely charged latex particles) and have been studied in some depth by the group here (1–3) and others (4, 5).

Some of the applications of the core/shell particles (Fig. 1a) are listed in Table 1. Microparticles with solid cores and shells have been prepared from the heteroaggregates described above (6–9) and also by other techniques (10–12). Core–shell particles with liquid cores and solid shells may be prepared by a number of means. Interfacial polymerization in emulsions (13–18) relies on monomers in the oil phase reacting at the o/w interface with monomers from the aqueous phase. As the shell is formed, the reaction rate is reduced, leading to relatively thin shells. Polymerization of certain vinyl monomers in emulsion droplets (which are immiscible with the resultant polymer) (19, 20) yields polymer that precipitates around the droplets as a shell under certain conditions. A small amount of unreacted monomer will always remain in the droplets, and may cause toxicity or odor problems. Coacervation (21–23) is the controlled precipitation of a polymer (or mixture of polymers) from the continuous (normally aqueous) phase of an emulsion around the droplets of the dispersed phase. This method suffers from lack of uniformity of the shell thickness, and is limited to shell polymers which are water-soluble. A recent development involves photopolymerization of monomers in the liquid shells surrounding the liquid cores of two-phase aerosol droplets (20). This led to monodisperse microcapsules with controlled shell thickness. The particles described were greater than 10 μm in diameter.

The method presented here leads to microcapsules with shells whose thickness (up to around 10% of the capsule radius) is a constant fraction of the capsule radius for all capsule sizes in the sample. Capsules below 10 μm are readily prepared. Although an older patent (24) has appeared which describes a similar approach, the authors are not aware of any systematic study in the open literature.

The basis of the method used here is shown schematically in Fig. 2. An o/w emulsion is first prepared which contains, as the oil phase, a mixture of polymer, a low-boiling good solvent for the polymer, and a high-boiling poor solvent for the polymer. Enough good solvent is present to ensure that the polymer is completely dissolved. A suitable emulsifier is employed in the aqueous phase, and the emulsion is formed by high shear stirring. The emulsion is then subjected to reduced pressure and elevated temperature which gradually removes the low-

[1] To whom correspondence should be addressed.

0021-9797/98 $25.00

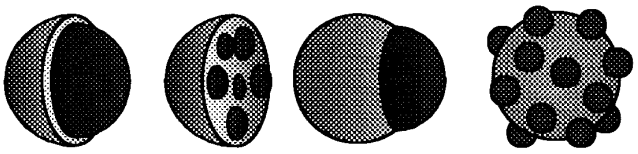

FIG. 1. Four possible two-phase particle morphologies: (a) core/shell, (b) occluded, (c) "acorn," and (d) heteroaggregate.

boiling solvent from the droplets. Eventually, when the droplet composition reaches the binodal boundary, the polymer phase separates as small droplets of liquid which are rich in solvent and polymer (called a coacervate phase) within the emulsion droplets. These coacervate droplets are mobile and migrate to the oil/water interface where they fuse and spread to engulf the original oil droplet if the wetting conditions are correct. Further solvent removal causes the polymer to precipitate at the interface, forming the shell.

BACKGROUND

Polymer Phase Separation in Mixed Solvents

The condition necessary for two phases to coexist in a three-component system is given by

$$\mu_i = \mu_i', \qquad [1]$$

where μ_i is the chemical potential of species i in the first phase and μ_i' is the chemical potential for the same species in the second phase. The classical Flory–Huggins theory (25) of solutions of polymers in binary solvent mixtures leads to

$$\mu_i - \mu_i^0 = RT\left[\ln v_i + (1 - v_i) - v_j\left(\frac{x_i}{x_j}\right) - v_k\left(\frac{x_i}{x_k}\right) + (\chi_{ij}v_j + \chi_{ik}v_k)(v_j + v_k) - \chi_{jk}\left(\frac{x_i}{x_j}\right)v_j v_k\right], \qquad [2]$$

where, for each species i, μ_i is the chemical potential (the superscript ^{0} denotes the standard state), v_i is the volume fraction, x_i is the number of segments, and χ_{ij} is the Flory interaction parameter between components i and j. RT takes its usual meaning. For the case of a polymer in a mixture of solvent and non-solvent (as was used in this study), the binodal conditions were calculated by Tompa (26). The resulting boundary curve in the ternary phase diagram separates the one-phase and two-phase regions.

Interfacial Spreading

Torza and Mason (27) have investigated the equilibrium morphology adopted by the droplets of immiscible liquids (phases 1 and 3) when brought into contact in a third mutually immiscible liquid (phase 2). For combinations of a range of liquids, the final equilibrium morphology was rationalized by analysis of the various interfacial tensions between the phases (γ_{12}, γ_{23}, and γ_{13}). By defining the spreading coefficients for each phase as

$$S_i = \gamma_{jk} - (\gamma_{ij} + \gamma_{ik}) \qquad [3]$$

and designating phase 1 to be that for which $\gamma_{12} > \gamma_{23}$, then $S_1 < 0$. It then follows that there are only three possible combinations of S_i,

$$S_1 < 0; \quad S_2 < 0; \quad S_3 > 0, \qquad [4]$$

$$S_1 < 0; \quad S_2 < 0; \quad S_3 < 0, \qquad [5]$$

$$S_1 < 0; \quad S_2 > 0; \quad S_3 < 0. \qquad [6]$$

When the conditions in Eq. [4] are satisfied the particles adopt a core–shell morphology (Fig. 1a) with phase 1 appearing as the core within a shell of phase 3. When Eq. [5] is satisfied, "acorn"-shaped particles (Fig. 1c) are formed, and when Eq. [6] is satisfied two separate droplets are preserved.

These ideas were used in the present study to rationalize the particle morphologies observed when the polymer was caused to phase separate within the emulsified droplets, with various core oil and aqueous emulsifier combinations. Although in this case one phase (the shell polymer) is eventually solid, the analysis is still valid since on phase separation the polymer phase is a solvent-rich liquid. This analysis was also applied successfully by Sundberg *et al.* in their experiments on *in situ* vinyl polymerization within non-solvent oil droplets (28).

EXPERIMENTAL

Materials

Methylmethacrylate (MMA, Aldrich, 99%) was distilled under vacuum prior to use. The polymerization solvent was THF (Fischer Scientific, 99%) and azobisisobutyronitrile

TABLE 1
Some Applications of Core/Shell Particles

Shell	Core	Application	References
Solid	Solid	Impact modifiers Drug release	(35, 36)
Solid	Liquid	Controlled release Oxidation prevention Perfume trapping Carbonless copy paper	(16, 23, 37, 38)
Liquid	Solid	Antifoams	—
Liquid	Liquid	Precursor	(27)

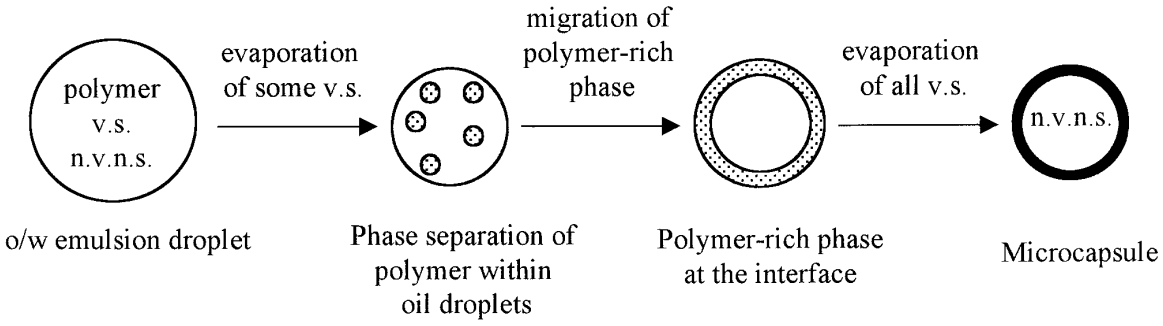

FIG. 2. Schematic of the steps involved in the encapsulation process: n.v.n.s., non-volatile non-solvent; v.s., volatile solvent.

(AIBN, BDH, 97%) was used as the initiator without further purification. Ethanol (Haymans, 99%) was used as polymer precipitant. Octanol (Aldrich, 99%), tetrachloromethane (BDH, 99.8%), hexadecane (HD, Aldrich, 99%), and decane (Aldrich, 99+%) were employed as core-oils. The *n*-alkanes were passed down a 30-cm column of neutral alumina (Aldrich, 95%) to remove impurities which have been shown to lower the oil–water interfacial tension (29, 30). Dichloromethane (DCM, Fischer Scientific, 99%) was used as polymer solvent. The emulsifiers used were poly(vinylalcohol) (PVA, 14,000 Da, 99% hydrolyzed, BDH), poly(methacrylic acid) (PMMA, BDH, 20% solution in water), poly(acrylic acid) (PAA, BDH, 25% solution in water), sodiumdodecylsulfate (SDS, Fluka, 99+%), and Cetyltrimethylammoniumbromide (CTAB, BDH, 98%). Ultrapure water (resistivity 18.2 MΩ cm) was provided by a Millipore "Milli-Q plus" unit.

Preparation of Poly(methylmethacrylate)

The poly(methylmethacrylate) used to form the microcapsule shells was synthesized by free-radical solution polymerization. A 1-L, round-bottomed flask equipped with a paddle agitator, reflux condensor, and nitrogen gas inlet was immersed in a thermostatted (±0.1°C) oil bath. THF (538 g) and MMA (178.15 g) were added, and the mixture was stirred under nitrogen for 20 min at 70°C to remove oxygen, then AIBN (0.90 g in 2.0 g THF) was added. The reaction was allowed to continue at 70°C for 21 h. The polymer was then precipitated by slowly pouring the solution into a fourfold excess of ethanol, with stirring, and was dried to constant mass in a vacuum oven at 40°C (~20 h).

Preparation of Microcapsules

The following method was used to prepare all microcapsules, although different amounts of polymer were used to vary the shell thickness. The method described here in detail is for the preparation of capsules whose shell thickness is one tenth of the microcapsule radius. PMMA (2.55 g) was dissolved in DCM (70.54 g) and then HD (3.865 g) was added. The relative amounts of each ingredient were chosen so that the system was in the one-phase region of the ternary phase diagram, and well away from the phase boundary.

For some preparations acetone was added to this solution in order to aid emulsification. An equal mass of aqueous surfactant solution was charged to a 200-ml jacketed glass vessel, maintained at 20°C (±0.5°C) by circulated water. The aqueous phase was stirred at 10,000 r.p.m. (Silverson stirrer), and the oil phase was added over 60 s to form an oil-in-water emulsion. Agitation was maintained at this rate for 1 h before pouring the emulsion into a further 120 mL of aqueous surfactant solution. This diluted emulsion was rotary evaporated for 20 min, with the temperature being ramped from 20 to 65°C over this time, after which the vacuum was turned off and the dispersion was maintained at 65°C for a further 40 min. The dispersion of microcapsules was cleaned by ultrafiltration using a Millipore Minitan unit equipped with 100 μm Minitan filter plates and fed by a Millipore variable-speed tubing-pump. The suspension was cleaned by repeated concentration/dilution, with a total of 10 L ultrapure water.

Characterization Techniques

Droplet size distributions of the various emulsions at different stages of homogenization were determined using a Coulter–Multisizer instrument, coupled to a PC running the analysis software version 4.1. Samples of the emulsions were diluted by a factor of approximately 2000 with Isoton (phosphate-buffered saline), and at least 100,000 droplets were counted in each run. A coincidence correction to account for the simultaneous measurement of two droplets was made automatically. The error arising from the correction was always below 2%.

Optical microscopy was performed using a Nikon Optiphot microscope fitted with Nikon ×20 and ×40 objective lenses. Micrographs were recorded using a Nikon PSM-3 flash unit on Ilford FP4 filmstock. A calibration grid with 20 μm spacings was photographed to calculate magnifications.

A Hitachi S-2300 scanning Electron Microscope was used to investigate the final microcapsule morphologies. One drop of the microcapsule dispersion to be investigated was placed on a stainless steel SEM stub and allowed to air-dry overnight.

Elevated temperatures and reduced pressures were avoided for this step in order to minimize loss of core oil by evaporation, since this could lead to deflation or some other distortion of the microcapsules. The dried sample was gold-coated in an Edwards S150A sputter coater. The chamber was evacuated to a pressure of approximately 0.8 kPa, and a sputtering current of 20 mA was applied for 4 min, giving a gold coating with a thickness of approximately 10 nm. To determine the polymer shell thickness, the microcapsules were fractured prior to gold-coating by applying direct pressure with a clean, round-tipped glass rod. To achieve brittle fracture of the capsules, the process was repeated under liquid nitrogen on freshly dried samples.

Ternary Phase Diagram

The ternary phase diagram for PMMA-HD-DCM was determined by mixing accurately weighed amounts of each material into 7-ml glass phials. The solutions were stirred by hand at ambient temperature to encourage the evaporation of the low-boiling DCM. When the solution started to appear cloudy due to polymer phase separation, the sample was reweighed. The loss in mass was attributed solely to the evaporation of the DCM, and the point in the phase diagram was determined by mass balance.

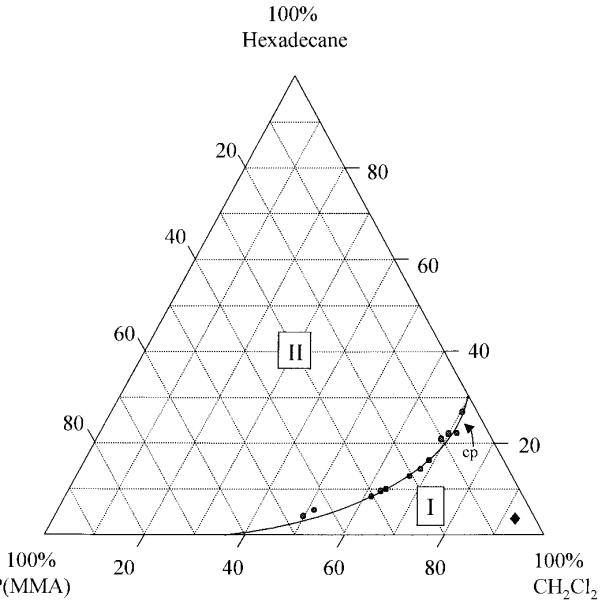

FIG. 3. Experimentally determined ternary phase diagram for the system PMMA/HD/CH_2Cl_2. The consolute point is marked "cp." The composition of the oil phase that was used to prepare microcapsules (when no acetone was used) is shown by ◆. I and II indicate the one-phase and two-phase regions, respectively. The axes are marked in wt%.

Interfacial Tensions

The interfacial tensions between the core-oils and the various aqueous surfactants were determined by the DuNuoy ring method using a Krüss Processor Tensiometer K12. The temperature was maintained at 20 (±0.2)°C by passing water from a thermostatted bath through a stainless steel collar around the measuring cup. Automatic measurements were made by pulling the ring through the interface from below, recording the mean of four measurements for each sample. The ring was cleaned in a Bunsen burner blue flame before use and also between samples.

Interfacial tensions between the PMMA and the various liquids were determined by measuring the contact angle (θ) of each liquid against a film of PMMA. The film had been deposited onto clean glass microscope slides from a 5% solution of PMMA in DCM. Contact angles were measured using a Krüss G2 system with G40 analysis software. At least four measurements were made for each liquid, and the mean contact angle was used to calculate the solid–liquid interfacial tension. The interfacial tensions between PMMA and the various liquids used was calculated from the mean contact angle using Young's equation

$$\gamma_{sv} = \gamma_{sl} + \gamma_{lv}\cos\theta, \qquad [7]$$

where γ is the interfacial tension between two phases and l, s, and v refer to liquid, solid, and vapor phases, respectively. The value of γ_{sv} for PMMA was taken as 41.1 mN m^{-1} from the literature (31), and γ_{lv} values were determined by the DuNuoy ring method as described earlier.

RESULTS AND DISCUSSION

Ternary Phase Diagram

The experimentally determined binodal for the HD/DCM/PMMA system is presented in Fig. 3. The important feature to note is that phase separation near the consolute point (marked cp), yields two phases which are both dilute in polymer. Since the polymer phase separates as a relatively dilute solution, it is able to spread over the remaining solvent-rich phase (the droplet) at the oil–water boundary. Spreading will occur when Eq. [4] is satisfied.

The two-phase systems on the binodal nearest the polymer corner of the diagram were very viscous. The implication of this in the formation of microcapsules is more fully discussed later.

Interfacial Tensions

The results of the surface and interfacial tension measurements are presented in Table 2, along with the calculated spreading coefficients and predicted and observed microcapsule morphologies.

During the contact angle measurements, the decane and octanol drops spread significantly on the PMMA film to such an extent that an accurate measurement of θ could not be made, but values were certainly less than 5°. In these cases, the

TABLE 2
The Interfacial Tensions, Contact Angles, and Spreading Coefficients Calculated for the Various Systems Under Study, According to Eqs. [4]–[6]

Oil (o)	Aq. emulsifier (w)	θ_{op} (degrees)	θ_{pw} (degrees)	γ_{ow} (mN m^{-1})	γ_{op} (mN m^{-1})	γ_{pw} (mN m^{-1})	S_1	S_2	S_3	Morphology	
										Predicted	Observed
HD	PMAA	17.3	71.4	35.4	14.6	18.9	<0	<0	>0	Core–shell	Core–shell
HD	PVA	17.3	65.6	21.6	14.6	18.8	<0	<0	<0	Acorn	Core–shell
HD	SDS	17.3	50.0	6.7	14.6	11.5	<0	<0	<0	Acorn	Acorn
HD	CTAB	17.3	38.3	<5[a]	14.6	13.1	<0	<0	<0	Acorn	Acorn
Decane	PMAA	<5	71.4	34.4	17.1	18.9	<0	<0	>0	Core–shell	Core–shell
Octanol	PMAA	<5	71.4	<5[a]	13.7	18.9	<0	<0	<0	Acorn	Acorn

[a] These interfacial tensions were too low to be measured by the DuNuoy ring method.

interfacial tensions were calculated as maximum possible values using a value for θ of 5°. Similarly, the interfacial tensions between HD and aqueous CTAB, and octanol and aqueous PMAA were too low to be measured by the DuNuoy ring method; the ring pulled through the interface. Since it was possible to measure an interfacial tension as low as 6.7 mN m^{-1}, it is safe to assume that any immeasurable interfacial tensions were less than this value, and 5 mN m^{-1} was arbitrarily chosen for the calculations.

Emulsion Droplet Size Distributions

The droplet size distributions of the emulsions prepared in this work are unlikely to change significantly with time due to Ostwald ripening (even on dilution), since each droplet contains the two highly water-insoluble species HD and PMMA. The presence of such species in the droplet phase of an emulsion has been shown to dramatically reduce the extent of Ostwald ripening (32, 33).

Effect of surfactant type. In this study, four emulsifiers were used to disperse the oil phase into water, PMAA, PVA, SDS, and CTAB. All emulsifiers were employed at a concentration of 1% by weight of aqueous phase. Attempts to emulsify the oil using PAA failed over a wide range of pH values, spanning the pK_a value of the of the polyacid (~4.5). This is attributed to its low affinity for the oil/water interface. The use of poly(vinylpyrolidinone) or poly(ethyleneoxide) led to gross coagulation during the solvent evaporation stage of the microcapsule synthesis.

TABLE 3
Droplet Diameters of the Emulsions Containing 3.1% PMMA and 0% Acetone, Made with Various Emulsifiers

Emulsifier	Mean droplet diameter (μm)
PMAA	7.67
PVA	26.52
SDS	10.05
CTAB[a]	1.21

[a] This value was measured by photo correlation spectroscopy.

The mean droplet diameters for the system containing 3.1% polymer and 0% acetone are presented in Table 3. Use of PVA yielded large droplets with a broad size distribution whereas PMAA and the smaller ionic surfactants yielded smaller droplets with a lower polydispersity. The emulsion prepared with CTAB as emulsifier had a much smaller mean droplet size than any of the other systems and a very narrow size distribution (polydispersity 0.07 by dynamic light scattering). These smaller droplet sizes are directly related to the fact that the oil–water interfacial tension was lowered by a much greater extent when ionic surfactants were employed (see Table 2). The droplets of emulsions prepared with PVA exhibit a certain degree of aggregation, indicating poorer colloidal stability with this emulsifier. Capsules formed from this emulsion are also highly aggregated, as will be discussed later.

Effect of acetone concentration in the oil phase. It has been reported previously (24) that the addition of a water-soluble co-solvent to an oil phase results in smaller droplets when this solution is emulsified. Figure 4 shows the droplet size distributions of emulsions containing 0, 5, and 10% acetone by weight, after 50 min emulsification. It is clear that increasing amounts of acetone not only reduced the average droplet diameter but also caused a narrowing of the droplet size distribution.

Effect of PMMA concentration in the oil phase. In order to make microcapsules with thinner shells, less PMMA was dissolved in the binary solvent mixture before emulsification. Droplet size distributions for emulsions containing 3.1, 1.2, and 0.2% PMMA in the oil phase are presented in Fig. 5. All oil phases contained 5% acetone and were emulsified for 60 min. It is clear that reducing the polymer concentration in the oil phase resulted in both the reduction in mean droplet diameter and a narrowing of the size distribution (although there is little difference between the results for 1.2 and 0.2% polymer). This is probably due to reduction of the oil phase viscosity with

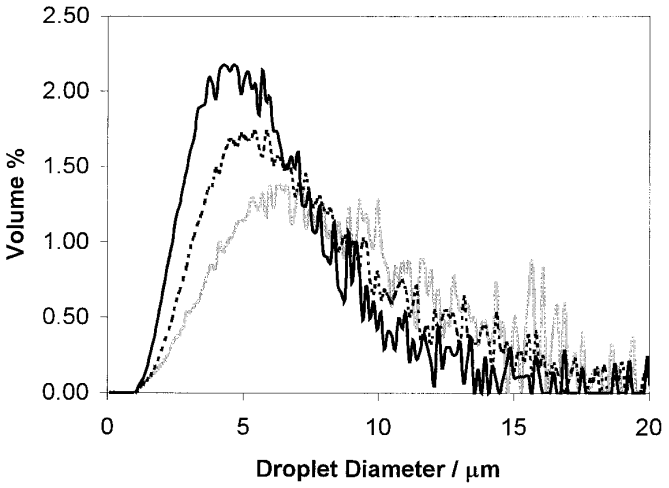

FIG. 4. Droplet size distributions of microcapsule pre-emulsions prepared using 3.1% PMMA in the oil, PMAA as emulsifier, and various concentrations of acetone in the oil phase.

lower polymer concentrations, facilitating the breakup of droplets during emulsification.

Microcapsule Morphologies

Capsule diameters. Since a single microcapsule is formed from each droplet, the particle size distribution of the microcapsule dispersion should exactly mirror that of the parent emulsion. The ratio of microcapsule diameter (d_{mc}) to parent droplet diameter (d_e) will be

$$\frac{d_{mc}}{d_e} = \left(\frac{v_p + v_{ns}}{v_p + v_{ns} + v_s}\right)^{1/3}, \qquad [8]$$

where v_p is the volume of polymer, v_{ns} the volume of non-solvent, and v_s the volume of good solvent in each droplet in the parent emulsion. For the emulsions prepared in this study, the removal of DCM should lead to a reduction in droplet diameter by a factor of two. However, when measured, the capsules prepared according to the method described in the experimental section (with 5% acetone), were only a factor of approximately 1.20 smaller than their parent emulsion droplets. This indicates that some droplet coalescence probably takes place after emulsion formation and before the capsules are formed.

As described in the background section, the equilibrium morphology of a composite particle is determined by the various interfacial tensions present during synthesis. The type of emulsifier and/or core oil determines these interfacial tensions. Results for the various systems used here are summarized in Table 2, along with the sign of the derived spreading coefficients calculated according to Eqs. [4]–[6]. It is clear that only the alkane/PMAA systems are expected, on this basis, to give rise to core/shell particles.

The fact that microcapsules contained HD is demonstrated in Fig. 6. A large capsule has been ruptured under the capillary pressure caused by drying the dispersion under a microscope cover slip. The oil has been forced out of the capsule center to form a pool (arrowed) alongside the capsule remnant.

Effect of emulsifier type. Although some "acorn" particles were observed in the HD/PVA system as predicted from the spreading coefficients, in the main spherical particles were observed. It is not clear why the predicted morphology was not dominant in this case, although Torza *et al.* (27) noted similar discrepancies in their work. The capsules prepared with PVA as emulsifier had uneven surfaces, and this will be discussed later.

The morphology of the particles prepared from emulsions containing SDS are shown in Fig. 7. The two-phase particles clearly have the "acorn" morphology, as predicted from the spreading coefficient analysis. One lobe of each particle was HD and the other lobe PMMA. The particles produced with CTAB as emulsifier had the same morphology (although smaller and less polydisperse), with the two halves of the "acorn" eventually separating to form individual particles. The PMMA particles then sedimented and the HD droplets creamed. It is not surprising that both acorn and (eventually) totally separated particles are observed in this system since $S_2 \approx 0$. It is quite possible that the "acorn" particles initially observed are kinetically favored, and slow rearrangement of the two lobes of the acorn leads to the final, fully separated system.

Effect of core oil type. So far all of the systems discussed contained HD as the polymer non-solvent, which became the core of the microcapsules. Other liquids were also investigated. When decane was used as the core oil, the same morphology as that observed for HD was predicted and observed. When tetrachloromethane was used, spherical particles were produced, but were

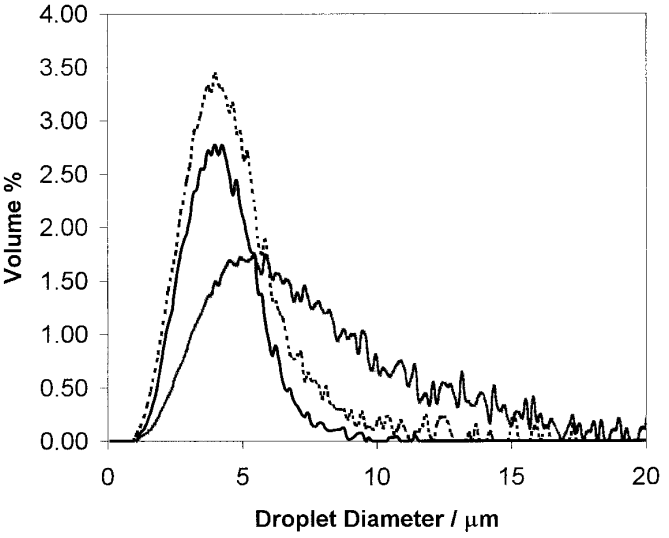

FIG. 5. Droplet size distributions of microcapsule pre-emulsions prepared with 5% acetone in the oil, PMAA as emulsifier, and various concentrations of PMMA in the oil phase.

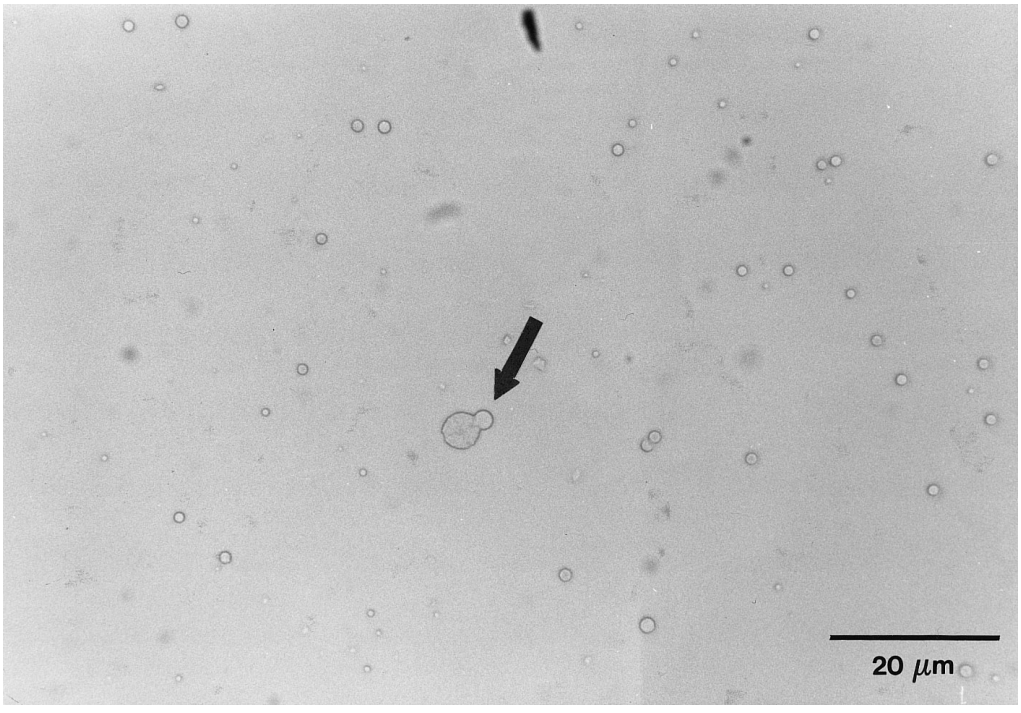

FIG. 6. Optical photomicrograph of a dried capsule dispersion showing a ruptured capsule exuding hexadecane (hexadecane arrowed) phase.

found to be uniform throughout, not core/shell. This was due to the loss of tetrachloromethane along with the DCM under the mild vacuum conditions in the rotary evaporator, leaving only solid polymeric spheres. This highlights the necessary condition that the core oil must be a reasonably high-boiling liquid (the boiling point of tetrachloromethane is 77°C compared to 174°C for de-

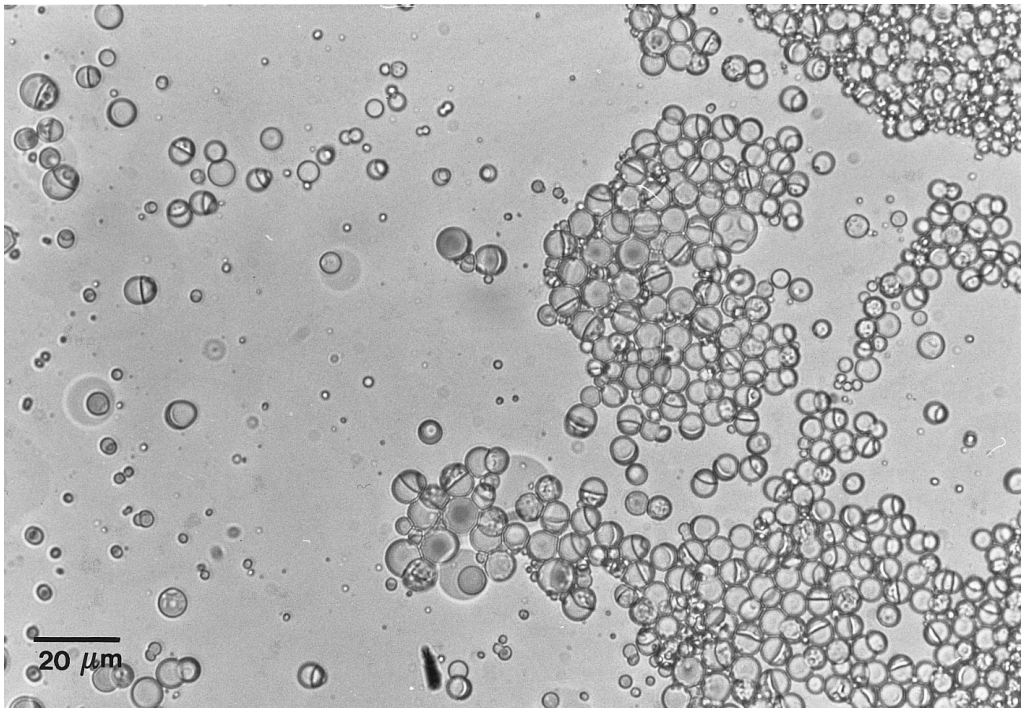

FIG. 7. Optical photomicrographs of the two-phase particles produced on phase separation in pre-emulsions prepared with HD as core oil, 3.1% PMMA, and 0% acetone in the oil phase, with SDS as emulsifier.

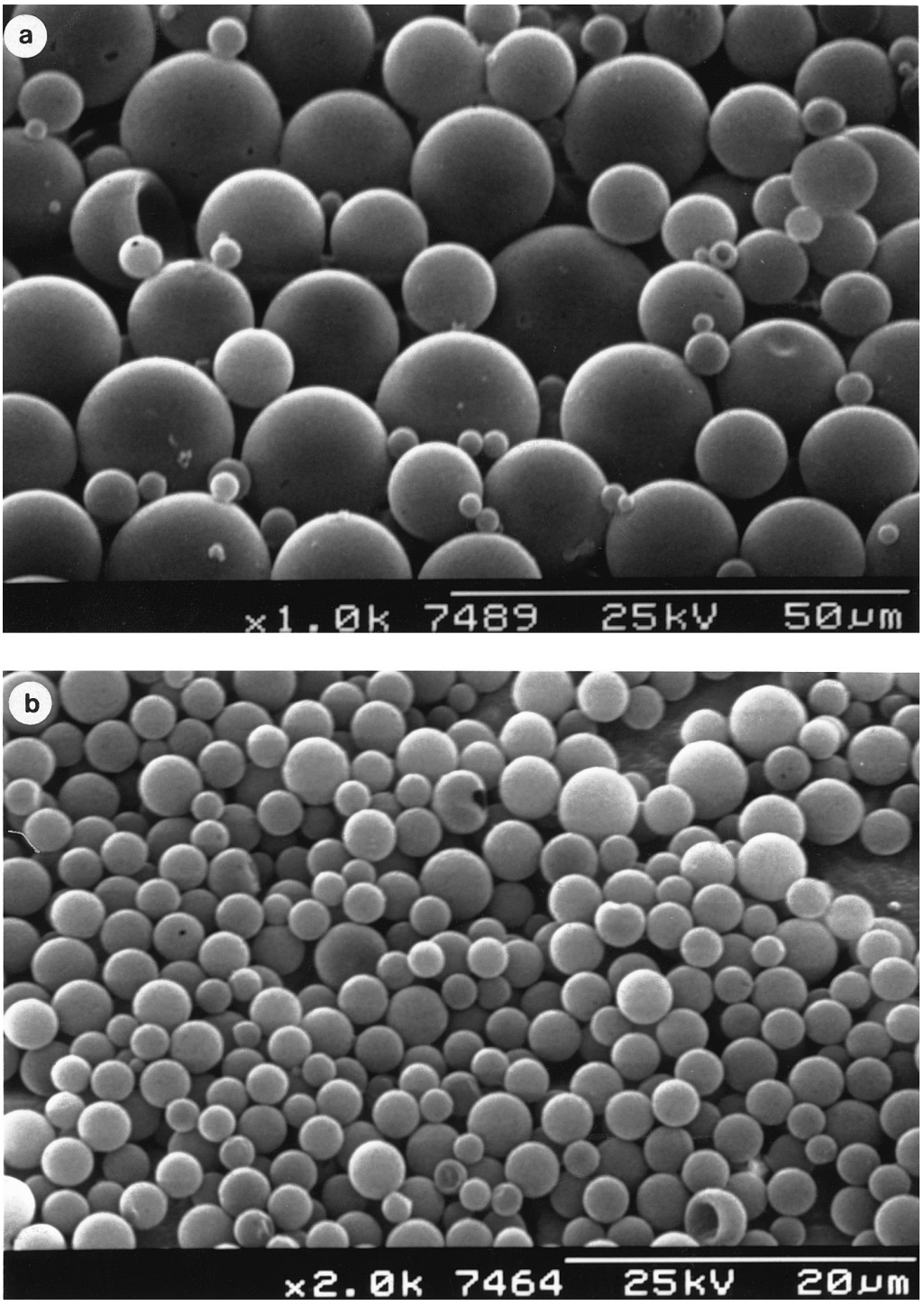

FIG. 8. Electron micrographs of microcapsules produced from pre-emulsions containing 3.1% PMMA in the oil, PMAA as emulsifier, and various acetone concentrations in the oil phase: (a) 0%; (b,c) 10%.

cane and 287°C for HD). Octanol (b.pt. 196°C) was also investigated as the core oil using PMAA as the emulsifier. The particles produced were again "acorn"-like as predicted. In this case the determining factor was the low interfacial tension between octanol and the aqueous phase.

Scanning electron microscopy. Electron micrographs of the microcapsules formed from emulsions prepared with PMAA as emulsifier, and oil phases containing 3.1% PMMA and either 0 or 10% acetone are presented in Fig. 8(a–c. The capsules were clearly spherical and those in Figs. 8a and 8b

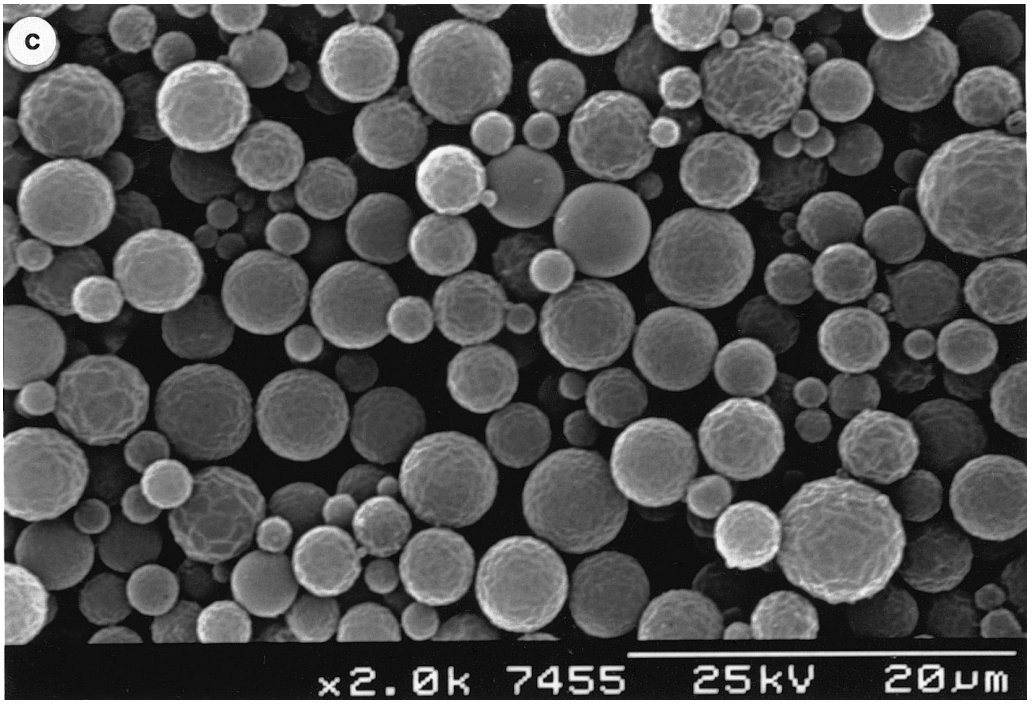

FIG. 8—*Continued*

had smooth surfaces (at this magnification). The diameters decreased with increasing acetone content as was observed for the parent emulsions, and the polydispersity was also reduced at higher acetone concentrations. The size and polydispersity of the microcapsules prepared with 5% acetone was between those of the 0 and 10% samples.

Some of the capsules in Fig. 8a have indentations on the surface. This has been observed by other workers (20, 28) and

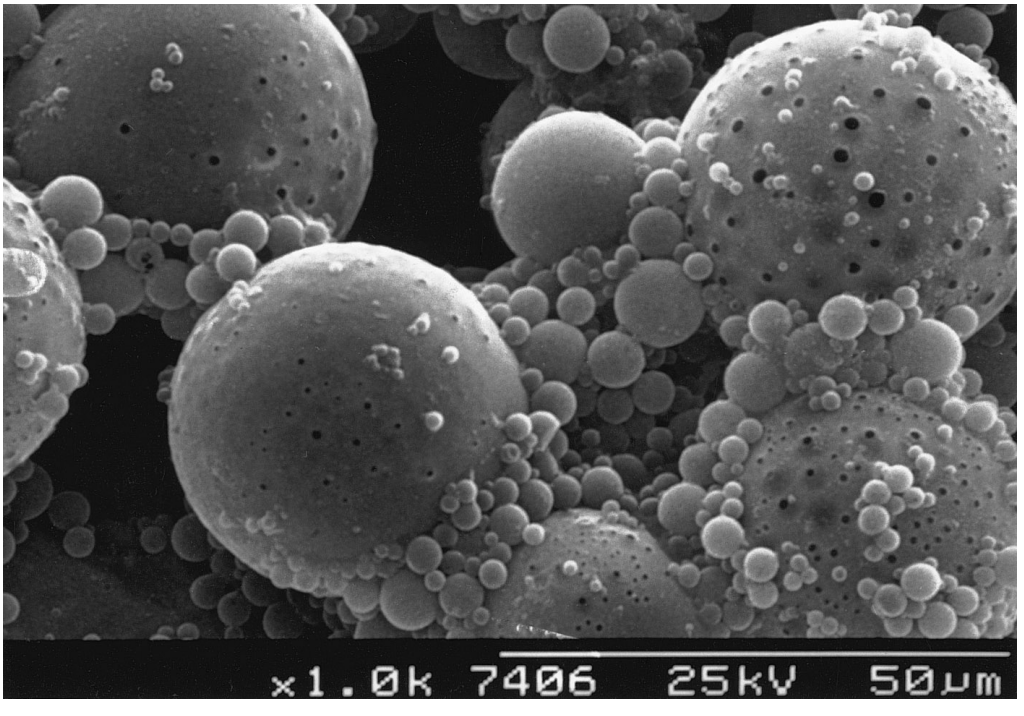

FIG. 9. Electron micrograph of microcapsules produced from a pre-emulsion containing 3.1% PMMA in the oil and PVA as emulsifier.

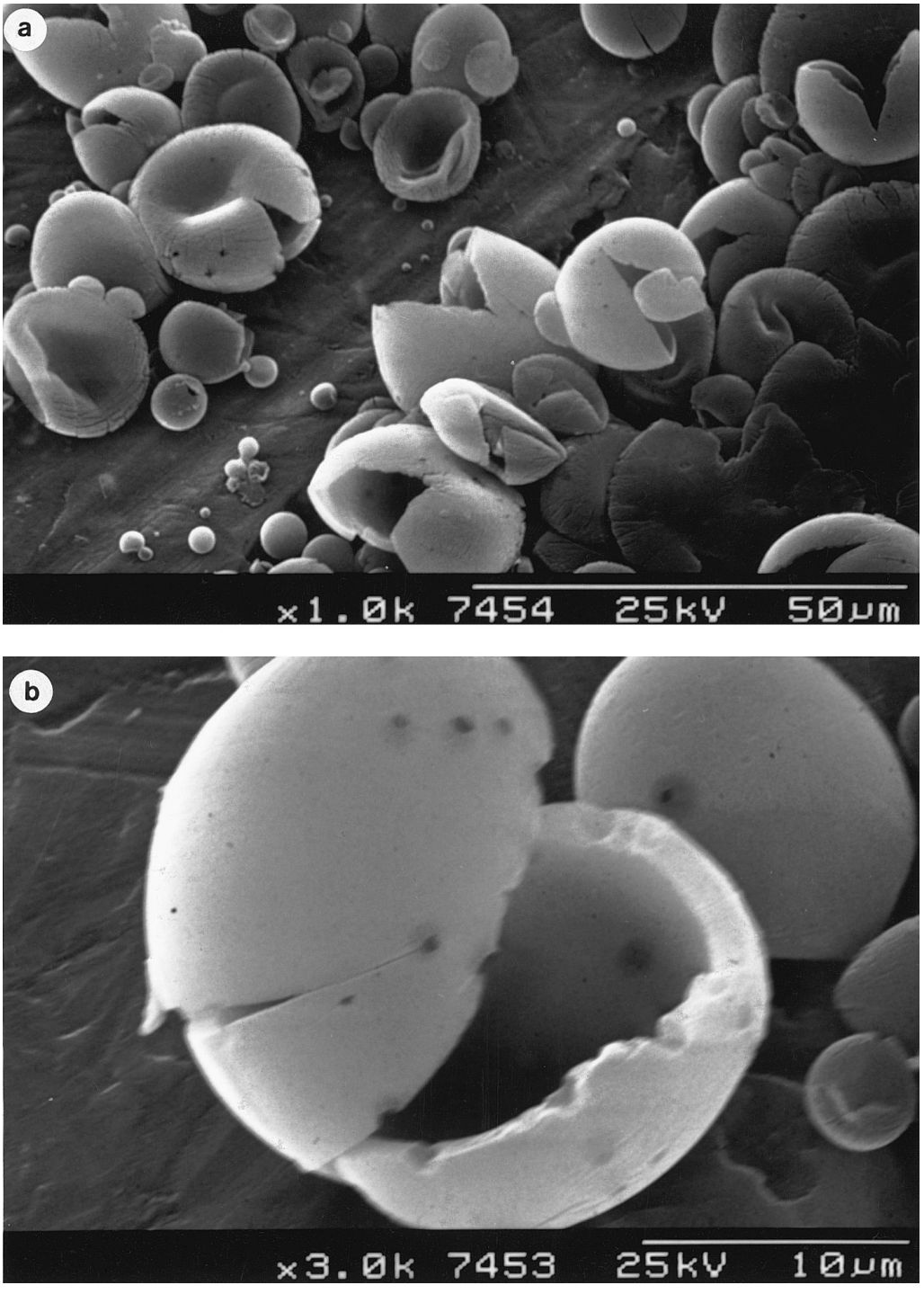

FIG. 10. Electron micrographs of fractured microcapsules produced from pre-emulsions containing 3.1% PMMA in the oil, PMAA as emulsifier, and various acetone concentrations in the oil phase: (a,b) 0%; (c) 5%.

was explained in terms of capsule collapse at shell thin-spots under the high vacuum required for SEM sample preparation (20), or interfacial tension gradients during synthesis (28). We favor the latter explanation, since the surface depressions were also observed under the optical microscope where the only reduction in pressure experienced by the capsules was that used in the rotary evaporator. The microcapsules illustrated in Fig. 8a and 8b were prepared immediately after the 60-min emulsification period. When microcapsules were prepared from an aged emulsion, the surfaces were quite uneven. A representative micrograph of capsules prepared from an emulsion that was stirred at 200 r.p.m. for 24 h after emulsification is pre-

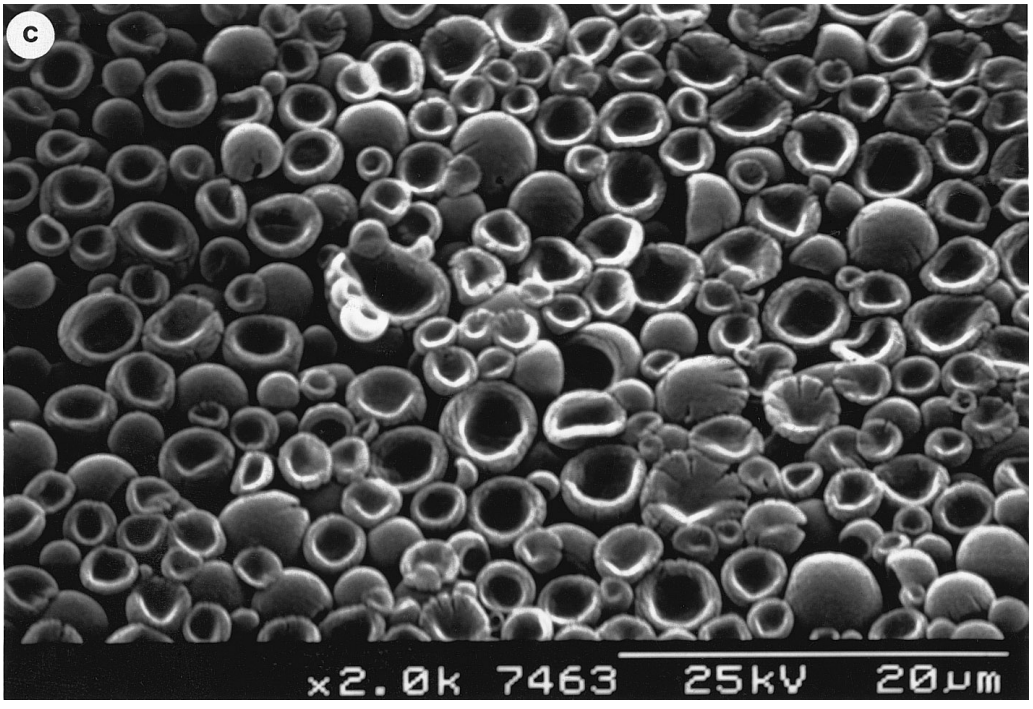

FIG. 10—*Continued*

sented in Fig. 8c. The difference in morphology may be explained on kinetic grounds. During the long stirring time after emulsification, the solvent evaporated slowly from the droplets causing them to shrink much more slowly than occurred in the rotary evaporator. Slow polymer phase separation at the interface then yielded an initially thin shell before the droplets had significantly shrunk. As more solvent was lost, and the droplets shrank further, the polymer skin was forced to buckle. Further polymer phase separation on the inside of the shell effectively froze the structure into that observed. This "brain-skin" morphology has been observed previously for poly(pyrrole) films which had undergone contraction (34).

Capsules prepared using PVA as emulsifier are very polydisperse, as shown in Fig. 9. It can also be seen that there were holes in the particle surfaces for the large particles. It would seem that solvent loss through the (thicker) shells of larger particles is by the eruption of liquid "bubbles" through the shell. Extensive aggregation has also occurred, highlighting the poor colloidal stability conferred by PVA.

In order to investigate the internal structure of the microcapsules shown in Figs. 8a and 8b, and to estimate their shell thickness, they were fractured as described in the experimental section. Micrographs of the fractured capsules are presented in Fig. 10. The large capsules shown in Fig. 10a, which were prepared in the absence of acetone, split open on fracture to reveal a single internal cavity (previously occupied by HD) which is shown more clearly in Fig. 10b at higher magnification. Examination of this micrograph yielded a ratio of shell thickness to microcapsule radius of almost 10%, as predicted.

Microcapsules made with acetone added to the oil phase collapsed rather than split, as shown in Fig. 10c for the 5% acetone sample. The same morphology was observed for the 10% acetone sample. It is possible that this is due to the smaller capsule size since the smallest capsules in Fig. 10a also seemed to fail in this way. Another explanation may be the plasticizing effect on the polymer shell of residual acetone, or even the core oil (HD). For this reason, the microcapsules prepared with 5% acetone were fractured under liquid nitrogen in order to encourage brittle failure of the shells. The results of this experiment are presented in Fig. 11. The same internal morphology as shown in Figs. 10a and 10b is observed, and the shell thickness as a fraction of the microcapsule radius appears similar for all samples at ~10%.

Variation of shell thickness. As stated previously, lowering the polymer content of the oil phase before emulsification should produce thinner shells. On the basis of the conservation of volume, for a capsule of radius r and shell thickness t, the ratio of the volume occupied by the shell (v_s) to the total capsule volume (v_t) is given by

$$\frac{v_s}{v_t} = \frac{r^3 - (r - t)^3}{r^3}. \qquad [9]$$

The volume fraction of polymer within the *non-volatile* oil $\phi_p = (v_s/v_t)$. (Note that ϕ_p is *not* the volume fraction of polymer in the droplets of the emulsion before solvent evaporation, when a large amount of solvent is present). Thus from Eq. [9]

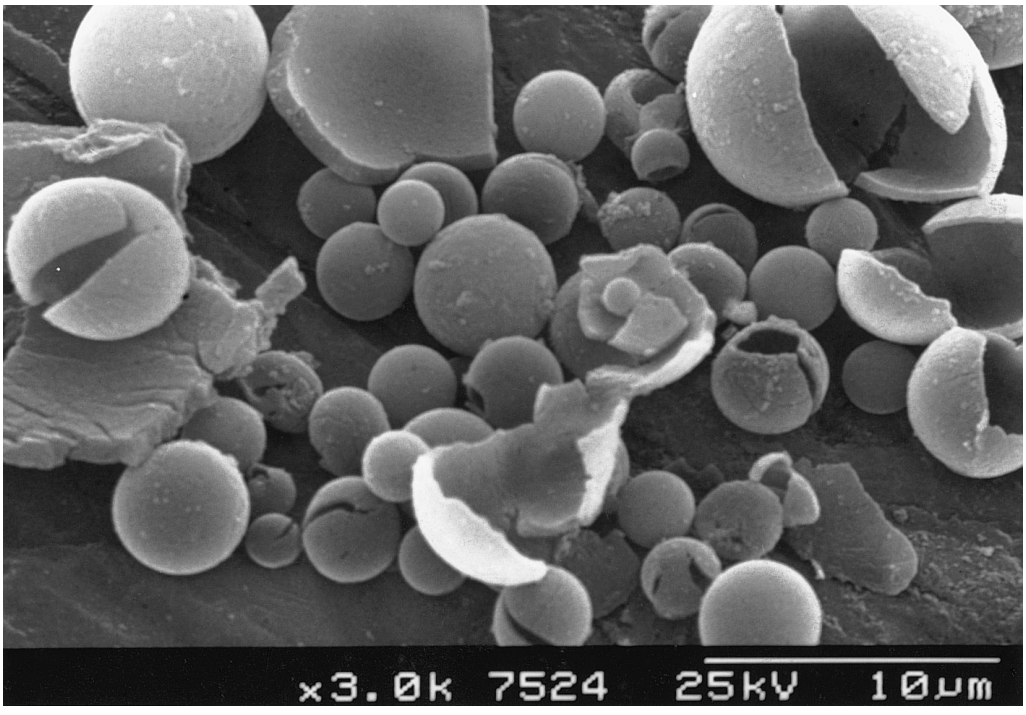

FIG. 11. Electron micrographs of the same microcapsules shown in Fig. 10c, but fractured under liquid nitrogen.

$$\phi_p = 1 - \frac{(r-t)^3}{r^3}, \qquad [10]$$

which rearranges to give

$$t/r = 1 - (1 - \phi_p)^{1/3}. \qquad [11]$$

This function is plotted in Fig. 12 and shows that in order to produce capsules with, for example, shells that are 50% of the overall capsule radius, the ratio of polymer to non-volatile core oil must be 85:15. During solvent removal and phase separation, this polymer concentration would yield highly viscous droplets (whose composition would cross the binodal near the polymer corner of the phase diagram). Thus, phase separation of the polymer, and spreading of the new phase over the droplet to form the shell, would be hindered. The occluded morphology of Fig. 1b with small HD droplets dispersed within a PMMA matrix would be expected in this case, though no experiments were conducted to confirm this. Instead, ϕ_p was kept below 0.3 yielding shells with thicknesses of $r/10$ or less.

Optical micrographs of capsules prepared from emulsions with 5% acetone and either 1.2% PMMA ($\phi_p = 0.2$) or 0.2% PMMA ($\phi_p = 0.045$) in the oil phase revealed spherical capsules, and both dispersions remained stable while in an aqueous environment. From Eq. [11], the predicted t/r values for these capsules is 5 and 1%, respectively, indicating that very thin shells can be formed using this technique. The electron micrographs of these particles are presented in Figs. 13a and 13b, respectively. It is clear that the shells were not strong enough, in either case, to withstand the SEM sample preparation conditions, and the capsules collapsed. Figure 13b shows the barely recognizable capsule remains when $\phi_p = 0.045$. However, analysis of these micrographs yields shell thicknesses which agree well with those predicted from Eq. [11].

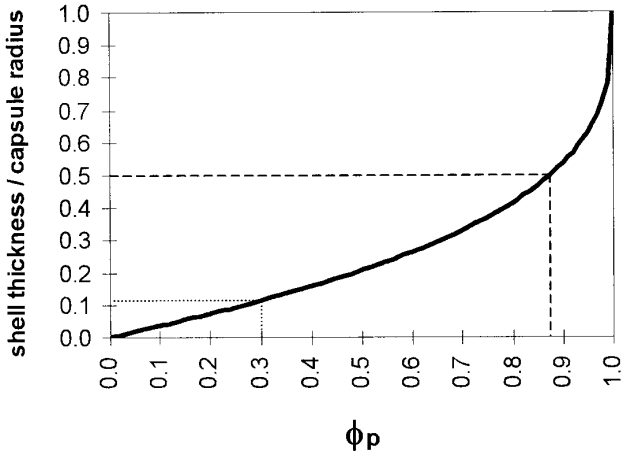

FIG. 12. A plot of (shell thickness/capsule radius) as a function of the volume fraction of PMMA in the capsule. (···) composition used in the majority of this study, (- - -) composition to give a ratio of shell thickness to capsule radius of 0.5 (see text).

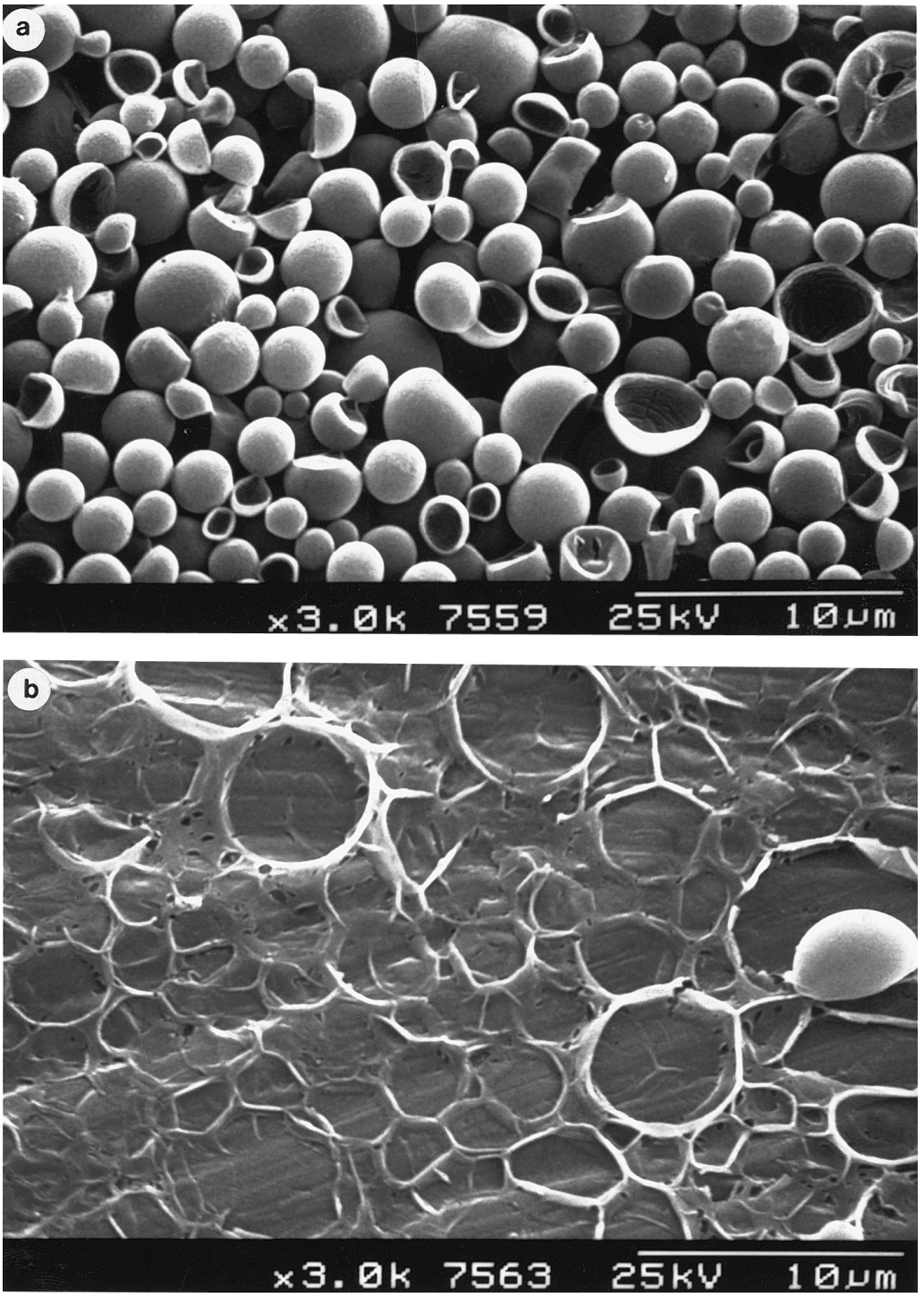

FIG. 13. Electron micrographs of microcapsules produced from pre-emulsions containing 5% acetone in the oil, PMAA as emulsifier, and two concentrations of PMMA in the oil phase: (a) 1.2%; (b) 1.2%. This should be compared with Fig. 8b, which shows the result for the 3.1% PMMA case.

CONCLUSIONS

It has been demonstrated that liquid–core/solid–shell particles can be prepared by phase separation within emulsion droplets. The morphology of the resultant particles is accurately predicted by analysis of the three spreading coefficients in the system.

Particles with liquid cores and polymeric shells were produced when the core oil had a high boiling point (for example

higher alkanes), and the spreading coefficients obey the inequalities in Eq. [4]. The latter condition was usually met when the interfacial tension between the core oil and aqueous phase is high. Octanol has a high boiling point, but a low interfacial tension with water, whereas tetrachloromethane has a relatively low boiling point and a high interfacial tension with water. Both oils were demonstrated to be unsuitable for producing core/shell particles by this method, underlining the importance of boiling point and o/w interfacial tensions.

Small ionic surfactants are unsuitable emulsifiers for forming core/shell particles by this method, as they reduce the oil–water interfacial tension by too great an extent, and yield "acorn" particles. The polymeric emulsifiers worked well, but gave slightly larger and more polydisperse droplets. The use of PVA leads to poor colloidal stability of the resultant microcapsule dispersion.

Capsules with shells of various thicknesses can be prepared by changing the concentration of polymer in the oil phase before emulsification. Shell thickness can be estimated by examination of scanning electron micrographs of fractured capsules, which is most readily carried out on capsules fractured at liquid nitrogen temperatures. Shell thickness was satisfactorily predicted on conservation of volume grounds.

ACKNOWLEDGMENT

The authors would like to thank the EPSRC for financial support.

REFERENCES

1. Harley, S., Thompson, D. W., and Vincent, B., *Colloids Surf.* **62,** 163 (1992).
2. Luckham, P. F., Vincent, B., McMahon, J., and Tadros, T. F., *Colloids Surf.* **6,** 83 (1983).
3. Vincent, B., Young, A., and Tadros, T. F., *J. Chem. Soc. Faraday Trans.* **65,** 296 (1978).
4. Dumont, F., Ameryckx, G., and Watillon, A., *Colloids Surf.* **51,** 171 (1990).
5. Okubo, M., He, Y., and Ichikawa, K., *Colloid Polym. Sci.* **269,** 125 (1991).
6. Okubo, M., Ichikawa, K., Tsujihiro, M., and He, Y., *Colloid Polym. Sci.* **268,** 791 (1990).
7. Okubo, M., Miyachi, N., and Lu, Y., *Colloid Polym. Sci.* **272,** 270 (1994).
8. Ottewill, R. H., Schofield, A. B., and Waters, J. A., *Colloid Polym. Sci.* **274,** 763 (1996).
9. Ottewill, R. H., Schofield, A. B., Waters, J. A., and Williams, N. S. J., *Colloid Polym. Sci.* **275,** 274 (1997).
10. Chen, Y. C., Dimonie, V., and Elaasser, M. S., *J. Appl. Polym. Sci.* **42,** 1049 (1991).
11. Chen, Y. C., Dimonie, V., and Elaasser, M. S., *J. Appl. Polym. Sci.* **46,** 691 (1992).
12. Pekarek, K. J., Jacob, J. S., and Mathiowitz, E., *Adv. Materials* **6,** 684 (1994).
13. Dobashi, T., Yeh, F. J., Ying, Q. C., Ichikawa, K., and Chu, B., *Langmuir* **11,** 4278 (1995).
14. Ichikawa, K., *J. Appl. Polym. Sci.* **54,** 1321 (1994).
15. Mahabadi, H. K., Ng, T. H., and Tan, H. S., *J. Microencapsulation* **13,** 559 (1996).
16. Okahata, Y., Noguchi, H., and Seki, T., *Macromolecules* **20,** 15–21 (1987).
17. Arshady, R., *J. Controlled Release* **14,** 111 (1990).
18. Arshady, R., *Polym. Eng. Sci.* **30,** 915 (1990).
19. Berg, J., Sundberg, D., and Kronberg, B., *Abstr. Papers Am. Chem. Soc.* **191,** 91-PMSE (1986).
20. Esen, C., Kaiser, T., Borchers, M. A., and Schweiger, G., *Colloid Polym. Sci.* **275,** 131 (1997).
21. Arshady, R., *Polym. Eng. Sci.* **30,** 905 (1990).
22. Burgess, D. J., Merak, T. A., Kwok, K. K., and Singh, O. N., *Abstr. Papers Am. Chem. Soc.* **201,** 320-POLY (1991).
23. Meyer, A., *Chimia* **46,** 101 (1992).
24. Baum, G., Bachmann, R., and Sliwka, W., (BASF), Microcapsules and Their Production, U.K. Patent 1,375,118, 1974.
25. Flory, P. J., "Principles of Polymer Chemistry." Cornell Univ. Press, London, 1953.
26. Tompa, H., *Trans. Faraday Soc.* **45,** 1142 (1949).
27. Torza, S., and Mason, S. G., *J. Colloid Interface Sci.* **33,** 67 (1970).
28. Berg, J., Sundberg, D., and Kronberg, B., *J. Microencapsulation* **6,** 327 (1989).
29. Aveyard, R., and Hayden, D. A., *Trans. Faraday Soc.* **61,** 2255 (1965).
30. Goebel, A., and Lunkenheimer, K., *Langmuir* **13,** 369 (1997).
31. Wu, S., *J. Phys. Chem.* **74,** 632 (1970).
32. Higuchi, W. I., and Misra, J., *J. Pharmaceut. Sci.* **51,** 459 (1962).
33. Davies, S. S., and Smith, A., *in* "Theory and Practise of Emulsion Technology" (A. L. Smith, Ed.), pp. 305. Academic Press, San Diego, 1976.
34. Saunders, B. R., Murray, K. S., Fleming, R. J., Cervini, R., and Allen, N. S., *in* "Handbook of Organic Conducting Molecules and Polymers" (H. Singh, Ed.), Vol. 3, Ch. 12. Wiley, London, 1997.
35. Schneider, M., Pith, T., and Lambla, M., *Polym. Adv. Technol.* **6,** 326 (1995).
36. Mathiowitz, E., Saltzman, W. M., Domb, A., Dor, P., and Langer, R., *J. Appl. Polym. Sci.* **35,** 755–774 (1988).
37. Goldner, H., *R&D Mag.* **36,** 137 (1994).
38. Brynko, C., (National Cash Register Company), Oil Containing Capsules and Method of Making Them, U.S. Patent 2,969,330, 1958.